Fast and Tunable Synthesis of ZrO_2 Nanocrystals: Mechanistic Insights into Precursor Dependence

Katrien De Keukeleere[†], Jonathan De Roo[†‡§], Petra Lommens[†], José C. Martins[§] and Isabel Van Driessche[†,*]

[†] Sol-gel Centre for Research on Inorganic Powders and Thin films Synthesis (SCRiPTS), Ghent University, Belgium

[‡] Physics and Chemistry of Nanostructures (PCN), Ghent University, Belgium

[§] NMR and structural analysis unit, Ghent University, Belgium

Keywords: *ZrO_2, nanocrystals, microwave, crystalline phases, reaction mechanism, phase transfer, NMR*

ABSTRACT: In this work, ZrO_2 nanocrystals (NCs) are synthesized via a solvothermal treatment in benzyl alcohol, which is an established method for the synthesis of many metal oxide nanocrystals. We found that the use of microwave heating allows for a reduction in reaction time from 2 days in the autoclave to merely 4 hours in the microwave. Furthermore, we were able to tune the crystallographic phase from pure cubic to pure monoclinic zirconia by changing the reaction mechanism through the use of a different zirconium precursor. Via GC-MS measurements we found that the release of a strong acid during synthesis controls the key mechanism behind the control over crystal phase formation. The as-synthesized ZrO_2 NCs (cubic or monoclinic) are small in size (3 – 10 nm), yet aggregated. However, aggregrate-free NCs are generated through a surface-functionalization with carboxylic acid ligands, providing stabilization in apolar solvents via steric hindrance. Solution ^{1}H NMR was used to study the details of this post-modification step and the surface chemistry of the resulting aggregate-free NCs. This led to the conclusion that not only a different crystal structure but also a different surface chemistry is obtained depending on the precursor composition.

INTRODUCTION

Zirconia can adopt three different crystalline phases, i.e. monoclinic (m), tetragonal (t) and cubic (c).[1] Depending on its crystalline phase, zirconia is used in numerous applications, e.g. c-ZrO_2 is applied in oxygen sensors, t-ZrO_2 is used as high performance transformation-toughened ceramics and can catalyze ethanol formation from syngas, while m-ZrO_2 will catalyze isobutanol formation from syngas and is important for gate dielectrics and bioactive coatings.[1-9] The tetragonal and cubic phase are not stable at room temperature under thermodynamic equilibrium, but they can be stabilized via the incorporation of divalent and trivalent cations (Mg^{2+}, Ca^{2+} …).[10, 11] Reducing the crystallite size of ZrO_2 below 30 nm can have the same effect.[10-12] Garvie et al. reported that this increased stability is due to a lower surface energy of the metastable phases of the nanocrystals (NCs) compared to the monoclinic phase.[13]

Various ZrO_2 synthesis methods are described in literature. Sol-gel methods and some solvothermal methods produce poorly crystalline particles and require an additional crystallization step at high temperatures, giving rise to highly agglomerated ZrO_2 NCs.[5, 14-19] Other methods suffer from the formation of mixed ZrO_2 phases[5, 20] and in general high temperatures and/or long reaction times[2, 4, 9, 21] are required. These drawbacks depend on a combination of different factors: the selected synthesis method, presence or absence of pressure, difference in precursor solution or pH… One of the most appealing synthesis routes was introduced by Niederberger et al. and uses a solvothermal autoclave method in benzyl alcohol to create a variety of crystalline metal oxide NCs (ZrO_2, HfO_2, In_2O_3, Ga_2O_3 …) at moderate temperatures.[22-25] This solvothermal method generally involves 2 days or more because heat transfer from the furnace to the steel autoclave vessel and the reaction mixture inside is slow. We explored if a microwave-assisted solvothermal treatment for ZrO_2 NCs results in NCs with identical properties in terms of diameter and crystallinity, yet at much shorter reaction times, since microwaves directly heat the precursor solution, resulting in faster and more homogenous heating.[26-28]

In the original benzyl alcohol synthesis, zirconium propoxide was used as a precursor to synthesize cubic ZrO_2 NCs. However, it has been shown before that the use of different precursor types can lead to different formation reaction mechanisms.[25, 29-31] For example, when using $TiCl_4$ for the synthesis of TiO_2 an alkyl halide elimination[32] takes place, while an ether elimination[29-31] arises when alkoxides precursors are used. Also in the microwave procedure described here a different reaction mechanism was found for different precursors. Moreover, detailed study led to the observation that the used precursor also leads to different crystalline ZrO_2 phases, implying that both phenomena are dependent on each other.

Here, XRD analysis was used to determine the crystalline ZrO_2 phase, while GC-MS analysis was applied to analyze the reaction mixtures to determine the reaction mechanism.

The as-synthesized ZrO_2 NCs are small in size (3 – 10 nm), aggregated and show low dispersibility in either polar or nonpolar solvents. However, aggregate-free NC

suspensions are required for implementations in most applications.[33] Some examples of surface post-modifications for NCs obtained via the benzyl alcohol route were described in literature for ZrO_2, HfO_2, Fe_3O_4 and ITO NCs.[22, 34-37] In general, aggregate-free NCs are generated via surface-functionalization with long chain ligands, providing stabilization via steric hindrance. We find that depending on the zirconium precursor used and the crystalline ZrO_2 phase formed, a different functionalization step is necessary. The cubic ZrO_2 NCs can be stabilized with the addition of only a long-chain carboxylic acid (e.g. oleic acid). The monoclinic ZrO_2 NCs on the other hand require a base (e.g. oleyl amine) in addition to the carboxylic acid. This again confirms that the use of a different precursor and thus a difference in reaction mechanism is of great influence as the obtained NCs not only differ in terms of crystallinity but also in surface chemistry. Solution ^{1}H NMR was used to study the details of the surface functionalization step and the surface chemistry of the resulting aggregate-free NCs.

EXPERIMENTAL

Materials. The following chemicals are purchased and used as such from Sigma Aldrich: zirconium(IV) chloride ($ZrCl_4$, ≥ 99.9 % trace metal basis), zirconium(IV) isopropoxide isopropanol complex ($Zr(OiPr)_4$, 99.9 % trace metal basis), zirconium(IV) ethoxide ($Zr(OEt)_4$, 97%), zirconium(IV) acetate ($Zr(Ac)_4$, in dilute acetic acid), benzyl alcohol (BnOH, anhydrous 99.8%), trifluoroacetic acid (TFA, 99%), oleic acid (OAc, technical grade 90%), oleyl amine (OAm, technical grade 70%) and dodecanoic acid (DDAc). Diethyl ether and ethanol (EtOH, dried) were used from Carl Roth and Merck respectively.

Nanocrystal synthesis. ZrO_2 nanocrystals were synthesized via a microwave-assisted solvothermal method. All precursor preparations were executed in a nitrogen filled glovebox, except for the acetate precursor. The zirconium precursor is brought into a 10 mL microwave vial together with 4.5 mL of BnOH, leading to a concentration of 0.13 M for all precursors (see Supporting Information).

actual treatment at temperatures between 220°C and 270°C.

Table 1 represents the different zirconium precursors. All precursor solutions are clear after 5 – 30 minutes of stirring, except the prop+H_2O and acetate precursor, showing precipitation and slight turbidity respectively. Every solution was subjected to a step-wise microwave treatment: a stirring step at 60°C and the
actual treatment at temperatures between 220°C and 270°C.

Table 1. Precursor compositions for the different zirconium sources.

Precursor label	Zirconium precursor
chloride	$ZrCl_4$
propoxide	$Zr(OiPr)_4$
prop+EtOH	$Zr(OiPr)_4$+EtOH
prop+H_2O	$Zr(OiPr)_4$+H_2O
prop+TFA	$Zr(OiPr)_4$+TFA
ethoxide	$Zr(OEt)_4$
acetate	$Zr(Ac)_4$

All precursor solutions give rise to a white precipitate and an organic supernatant after synthesis. However, the chloride, prop+H_2O and the prop+TFA precursors produce an additional water phase. The white precipitate is collected through centrifugation (2500 rpm, 2 min) and is washed up to three times with diethyl ether. The resulting precipitate is dispersed in ethanol for TEM analysis or dried at 60 °C for XRD analysis.

Surface functionalization. NCs obtained from the chloride and propoxide precursor were used for further functionalization in order to obtain clear colloidal NC suspensions. The washed NCs were redispersed in 4 mL of chloroform and 0.2 mmol of carboxylic acid (DDAc or OAc) was added to the milky suspension. A colorless, transparent suspension was obtained after 24 hours of stirring in case of the ZrO_2 NCs obtained from the propoxide precursor. The ZrO_2 NCs from the chloride precursor only formed a transparent and colorless suspension in chloroform if a base, i.e. OAm (0.15 mmol), was added in addition to the carboxylic acid.

Characterization. X-ray diffraction (XRD) was performed on a Thermo Scientific ARL X'tra X-ray diffractometer with the CuKα line as the primary X-ray source. The crystallite size is determined via the Scherrer equation using 0.95 as shape factor. Transmission electron microscopy (TEM) images were taken on a JEOL JEM-2200FS TEM with Cs corrector. STA 449 F3 Jupiter of Netzsch was used to perform thermogravimetrical analysis (TGA), to determine the yield of all syntheses. The TGA experiments were all conducted under air (120/50) with a rate of 10 K/min to 800°C. A Malvern Nano ZS in backscattering mode (173°) was used for Dynamic Light Scattering (DLS) measurements. Gas Chromatography – Mass Spectrometry (GC-MS) experiments were performed on a Hewlett Packard G1800B GCD. Nuclear Magnetic Resonance (NMR) measurements were recorded on a Bruker Avance III Spectrometer operating at a ^{1}H frequency of 500.13 MHz and equipped with a BBI-Z probe or on a Bruker Avance II Spectrometer operating at a ^{1}H frequency of 500.13 MHz and equipped with a ^{1}H, ^{13}C, ^{31}P TXI-Z probe. A 750 µL ampule of dry deuterated solvent was used for each NMR measurement and the sample temperature was fixed at 298.2 K. One dimensional (1D) ^{1}H and 2D NOESY (Nuclear Overhauser Effect Spectroscopy) spectra were acquired using standard pulse sequences from the Bruker library. For the quantitative 1D ^{1}H measurements, 64k data points were sampled with the spectral width set to 16 ppm and a relaxation delay of 30 seconds. The NOESY mixing time was set to 300 ms and 4096 data points in the direct dimension for 512 data points in the indirect dimension were typically sampled, with the spectral width set to 16 ppm.

Diffusion measurements (2D DOSY) were performed using a double stimulated echo sequence for convection compensation and with monopolar gradient pulses.[38] Smoothed rectangle gradient pulse shapes were used throughout. The gradient strength was varied linearly from 2-95% of the probe's maximum value (calibrated at 50.2 G/cm) in 32 or 64 steps, with the gradient pulse duration and diffusion delay optimized to ensure a final attenuation of the signal in the final increment of less than 10 % relative to the first increment. For 2D processing, the spectra were zero filled until a 4096×2048 real data matrix. Before Fourier transformation, the 2D spectra were multiplied with a squared cosine bell function in both dimensions, the 1D spectra were multiplied with an exponential window function. Concentrations were obtained using the Digital ERETIC method. The diffusion coefficients were obtained by fitting the appropriate Stejskal-Tanner equation to the signal intensity decay.[39]

RESULTS AND DISCUSSION

Conventional versus Microwave. We transferred the conventional solvothermal synthesis of ZrO2 NCs in benzyl alcohol, described by Garnweitner et al. [22, 28], to a microwave-assisted solvothermal synthesis to explore if the same results can be obtained in much shorter reaction times.

A two-step microwave treatment was performed on the propoxide precursor solution (

actual treatment at temperatures between 220°C and 270°C.

Table 1): 60°C for 5 minutes and 270°C for 4 hours. This microwave treatment resulted in crystalline c-ZrO2 NCs of 3 – 4 nm in diameter, according to the XRD diffractogram, SAED pattern and TEM image (**Figure 1**). The crystallite diameter is determined as 4.2 nm and the yield of this synthesis is gravimetrically determined as 97.7%.

Identical results in terms of crystalline phase and

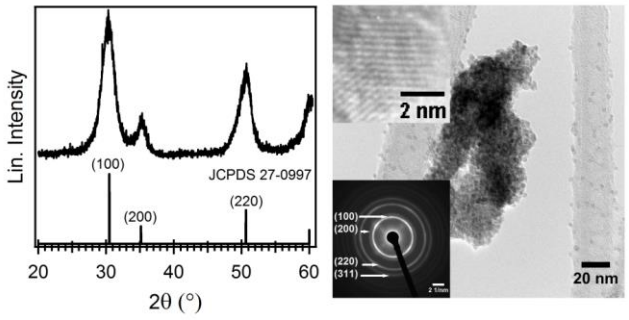

Figure 1. XRD diffractogram of c-ZrO_2 NCs (left) and (HR-)TEM with accompanying SAED pattern of c-ZrO_2 NCs (right) obtained from the propoxide precursor microwave treated at 270°C for 4 hours.

average diameter are obtained via the conventional solvothermal synthesis of zirconium propoxide, although a lower crystallite diameter of 2.8 nm is found.[22]

These results clearly show that by using a microwave-assisted solvothermal treatment instead of the conventional treatment one can drastically reduce the reaction time up to 12 times.

Precursor effect on crystalline phase. We examined if the use of different zirconium precursors for the microwave-assisted synthesis leads to different reaction mechanisms observed for other oxides, and if these differences result in NCs with varying properties.[25, 29-31]

The propoxide, chloride, ethoxide and acetate precursors were all subjected to a completely identical two-step microwave treatment – 60°C for 5 minutes and 230°C for 6 hours – to study their effect on the formation of the crystalline phases and reaction mechanisms during microwave synthesis. The propoxide precursor again leads to cubic ZrO_2 NCs with an average diameter of 3 nm. However, a decrease in synthesis temperature (230°C instead of 270°C) gives rise to a lower yield (

Also the second type of alkoxide precursor, ethoxide, and the acetate precursor lead to pure cubic ZrO2 NCs (Figure 2). However, the chloride precursor leads to

Table 2, **Figure 2** and **Figure 3**).

Also the second type of alkoxide precursor, ethoxide, and the acetate precursor lead to pure cubic ZrO_2 NCs (Figure 2). However, the chloride precursor leads to

Table 2. Overview of the maximum pressures reached during the microwave treatment at 230°C, crystalline phase of the ZrO_2 NCs, crystallite size d_{cryst} and yield for the corresponding precursor solutions.

Precursor label	Maximum pressure	Crystalline phase	d_{cryst}	yield
propoxide	2 bar	Cubic	3 nm	23 %
chloride	20 bar	Monoclinic	3.8 nm	95 %
ethoxide	2.1 bar	Cubic	3 nm	25 %
acetate	7.7 bar	Cubic	2.8 nm	47 %

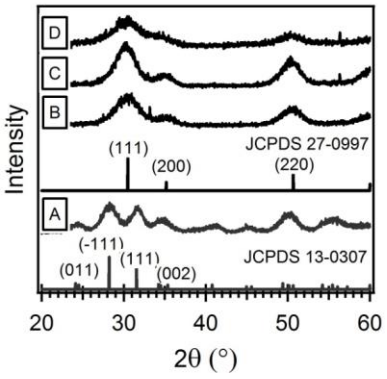

Figure 2. XRD diffractograms of m-ZrO_2 NCs (JCPDS card no. 13-0307) obtained from the chloride precursor (A) and c-ZrO_2 NCs (JCPDS card no. 27-0997) obtained after microwave treatment of the propoxide (B), ethoxide (C) and acetate (D) precursor solutions.

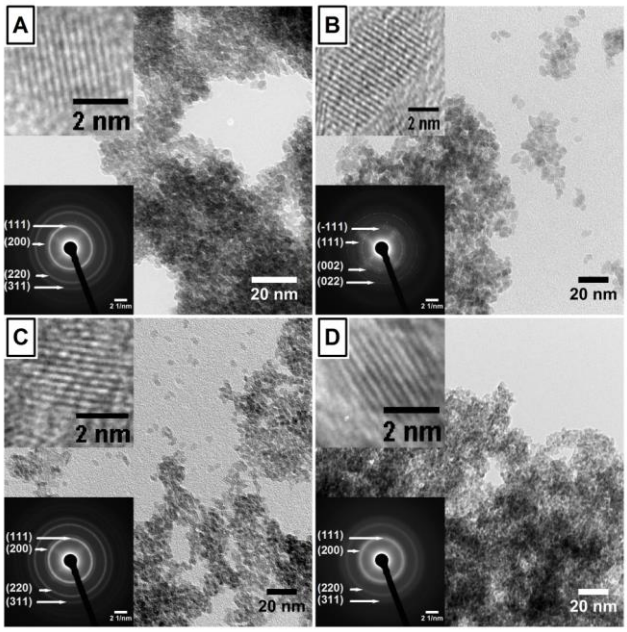

Figure 3. (HR-)TEM with accompanying SAED pattern of ZrO_2 NCs obtained from the propoxide (A), chloride (B), ethoxide (C) and acetate (D) precursor.

pure monoclinic ZrO_2 NCs, according to XRD analysis (**Figure 2**). (HR-)TEM analysis of the NCs obtained from the different precursors shows that all are crystalline and highly agglomerated, while the accompanying SAED patterns confirm the outcome of the respective XRD measurements (**Figure 3**). In
Also the second type of alkoxide precursor, ethoxide, and the acetate precursor lead to pure cubic ZrO2 NCs (Figure 2). However, the chloride precursor leads to
Table 2 it is also shown that the microwave treatment on the chloride precursor leads to almost full conversion (95%) while all others result in a yield below 50%.

Next to the change in crystalline phase obtained by switching from the propoxide to the chloride precursor, other important changes were observed during synthesis. First, the chloride precursor generates a much higher pressure during the microwave treatment (

Also the second type of alkoxide precursor, ethoxide, and the acetate precursor lead to pure cubic ZrO2 NCs (Figure 2). However, the chloride precursor leads to

Table 2). According to literature[40, 41], the obtained crystallographic ZrO_2 phase can depend on the applied pressure, however little is known on the influence of the pressure that arises during a solvothermal treatment on the ZrO_2 phase formation. An anhydrous alcohol was added to the propoxide precursor to raise to pressure of the system during microwave synthesis. We chose anhydrous ethanol, because it does not interfere in the reaction mechanism itself. From the resulting XRD and TEM analysis it is clear that the sole presence of a higher pressure (10 vs. 2 bar) does not lead to a crystal phase change of ZrO_2 (Table 3, **Figure 4** and SAED **Figure 5**A), but it does lead to an increased crystallinity and average diameter.

Second, a water phase is detected after the microwave treatment of the chloride precursor. It has been discussed before that the presence of water can facilitate the formation of m-ZrO_2 over c-ZrO_2.[16, 42] Water is believed to increase the solubility of the formed ZrO_2 precipitates during synthesis which facilitates the effective operation of dissolution and precipitation leading to the more stable m-ZrO_2.[16, 43-45] To assess the role of water in

Table 3. Overview of the maximum pressure reached during the microwave treatment, crystalline phase, crystallite size d_{cryst} and yield of the obtained ZrO_2 NCs obtained from the microwave treatment of the different precursor solutions.

Precursor label	Maximum pressure	Crystalline phase	d_{cryst}	Yield
prop+EtOH	10 bar	Cubic	3.7 nm	25 %
prop+H_2O	19.3 bar	Cubic	4.2 nm	84 %
prop+TFA	25 bar	Monoclinic	6.5 nm	100 %

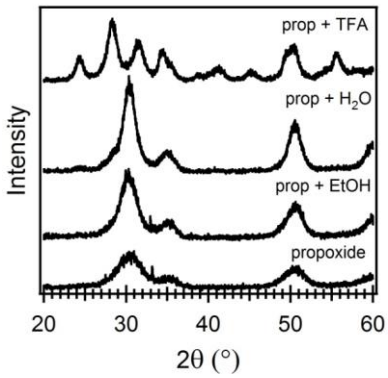

Figure 4. XRD diffractograms of ZrO_2 NCs obtained from the microwave treatment of the pure and the modified propoxide precursor (EtOH, H_2O and TFA).

in our synthesis method, distilled water was added to the propoxide precursor. From the resulting XRD and TEM analysis it is clear that the presence of water does not lead to a change in crystal phase of ZrO_2 (Table 3, **Figure 4** and SAED **Figure 5**B). Yet, the presence of water does lead to a higher pressure (19 vs. 2 bar) and an increased NC crystallinity.

Third, only the chloride precursor has the potential to form a strong acid (HCl) during hydrolysis. To assess the influence of the presence of a strong acid, trifluoroacetic acid (TFA) was added to the propoxide precursor. The addition of a strong acid to the propoxide precursor indeed leads to the formation of m-ZrO_2 instead of c-ZrO_2 (**Figure 4** and SAED **Figure 5**C).

These results suggest that the presence of a strong acid leads to a different reaction mechanism, releasing H_2O during synthesis, and causing the NCs to grow in a different crystal structure.

We used GC-MS analysis to study the composition of the different mixtures after microwave synthesis (see Supporting Information). The reaction mixture of the microwave treated propoxide precursor contained primarily benzyl alcohol and only in a small amount

dibenzyl ether. We suggest the following two-step mechanism:

$$Zr(OiPr)_4 + x\ BnOH \leftrightarrows Zr(OiPr)_{4-x}(OBn)_x + x\ HOiPr \quad (1)$$

$$2\ ZrR_3(OBn) \rightarrow ZrR_3\text{-}O\text{-}ZrR_3 + BnOBn \quad (2)$$

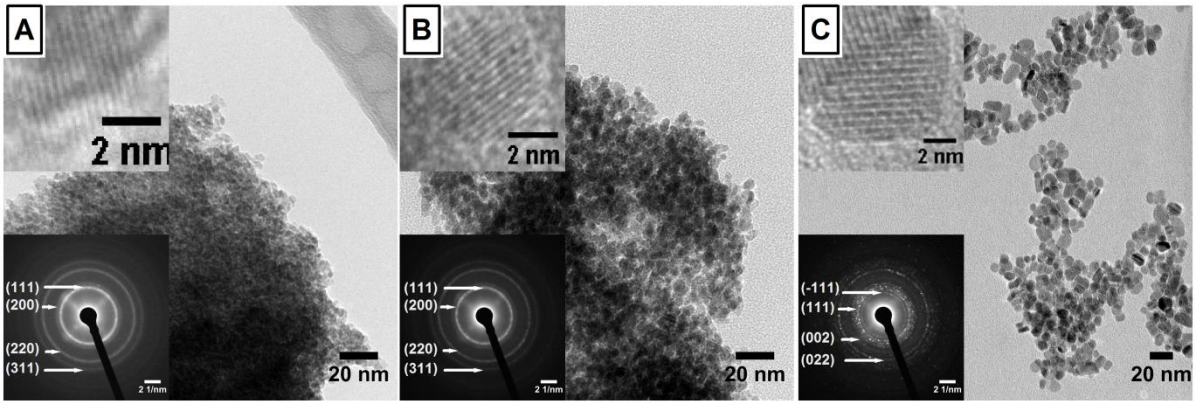

Figure 5. (HR-)TEM micrograhs with accompanying SAED pattern of ZrO_2 NCs from the prop+EtOH (A), prop+H_2O (B) and prop+TFA (C) precursors.

Ligands that are not participating in the reaction are denoted as 'R', with R = -OiPr or – OBn. Here, a ligand exchange takes place in the first step (1), where the propoxide is (partly) replaced by benzyl alcoholate. In the second step (2), an ether elimination takes place, forming dibenzyl ether and the oxygen-metal bound, leading to the final formation of ZrO_2 NCs. This mechanism is identical to the one suggested by Pinna *et al.* for HfO_2 nanocrystals with alkoxides as a reagent.[31]

The reaction mixture obtained after microwave treatment of the chloride precursor contained primarily dibenzyl ether and only a small amount of the original solvent, benzyl alcohol, remained. This suggests the occurrence of a different reaction, in which next to the typical ligand exchange (4) and ether elimination (5), a third reaction plays a role (6):

$$ZrCl_4 + x\ BnOH \leftrightarrows ZrCl_{4-x}(OBn)_x + x\ HCl \quad (4)$$

$$2\ ZrX_3(OBn) \rightarrow ZrX_3\text{-}O\text{-}ZrX_3 + BnOBn \quad (5)$$

$$2\ BnOH \xrightarrow{acid} BnOBn + H_2O \quad (6)$$

With 'X' denoting ligands that are not participating in the reaction (X = -Cl or –Obn). Reaction (6), the acid catalyzed condensation of benzyl alcohol, can only occur because of the presence of the HCl formed in-situ. This reaction transforms the benzyl alcohol in dibenzyl ether, explaining that in the case of $ZrCl_4$ only a small amount of the original solvent is left. On the other hand, when using the propoxide precursor, the solvent is only involved in the ligand exchange reaction. A similar mechanism was observed for the synthesis of HfO_2 NCs from $HfCl_4$ in BnOH using a microwave-assisted synthesis.[27]

The reaction mixtures of the prop+EtOH, prop+H_2O, ethoxide and acetate precursor are similar to the propoxide precursor, suggesting that only the ligand exchange and ether elimination takes place according to the first reaction scheme. The reaction mixture of the prop+TFA precursor on the other hand is similar to the chloride precursor, suggesting that also here the additional acid catalyzed condensation takes place (scheme 2). The in-situ release of acetic acid in the case of acetate precursor leads to c-ZrO_2 and not to m-ZrO_2. However, acetic acid, being a weak acid, will not catalyze the ether condensation and does not lead to m-ZrO_2 NCs. Thus, only the presence of the acid catalyzed condensation step gives rise to the formation of m-ZrO_2 NCs.

Precursor effect on stabilization and surface chemistry. In an effort to improve the colloidal stability of the different suspensions and to de-aggregate the as-synthesized NCs, a surface functionalization was executed. In this section, we will elaborate on this post-synthetic modification for the ZrO_2 NCs obtained from the propoxide precursor (c-ZrO_2) and the chloride precursor (m-ZrO_2). The microwave treatment on these precursors was optimized to obtain optimal post-modification conditions.

Propoxide precursor. The as-synthesized c-ZrO_2 NCs are aggregated, irrespective of the used microwave reaction conditions (4h 270°C vs. 6h 230°C), and lead to a turbid and unstable suspension after redispersion in chloroform (**Figure 6**A). The NCs can be stabilized with a long chain carboxylic acid (oleic acid in this case) , as described by Garnweitner *et al.* for ZrO_2 NCs synthesized via a conventional benzyl alcohol route, leading to a stable, clear and colorless suspension (**Figure 6**B).[22]

DLS measurements of these ZrO_2 NC suspensions obtained from for the precursor treated at 230°C for 6 hours confirms that the c-ZrO_2 NCs are aggregrate-free with an average solvodynamic diameter (d_s) of 11.7 nm. The treatment at 270°C for 4 hours gives rise to aggregate-free NCs with a similar d_s of 9 nm (**Figure 6**C). TEM micrographs in **Figure 6**D and E show that the NCs are indeed individual and spherical, irrespective of the microwave treatment used. On average, the NCs synthesized at a lower temperature are smaller (2.8 vs 4.7 nm in diameter).

The stabilizing role of the carboxylic acid is investigated by 1D ^{1}H NMR and 2D NOESY spectra on c-ZrO_2 NCs stabilized with oleic acid (OAc). Oleic acid was

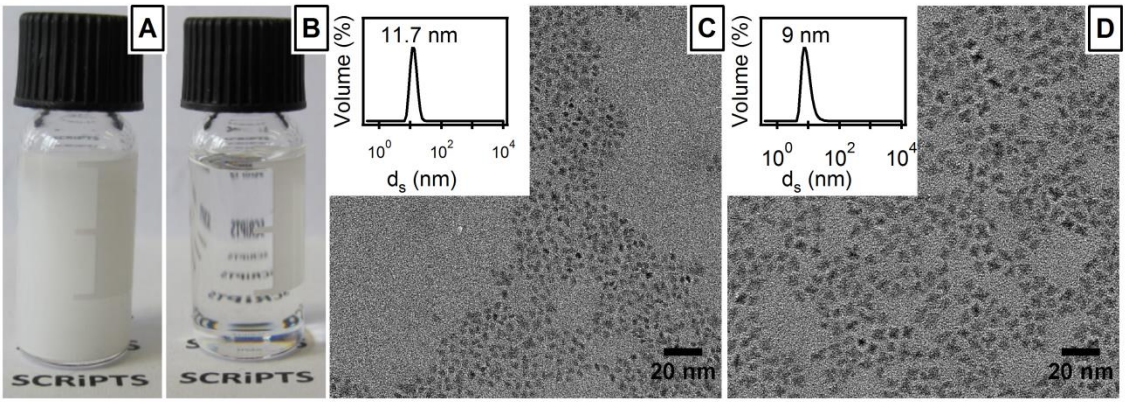

Figure 6. c-ZrO_2 NCs in chloroform before (A) and after (B) post-modification with oleic acid, DLS and TEM micrograpahs of the post-modified c-ZrO_2 NCs starting from the propoxide precursor microwave treated at 230°C for 6 hours (C) or 270°C for 4 hours (D).

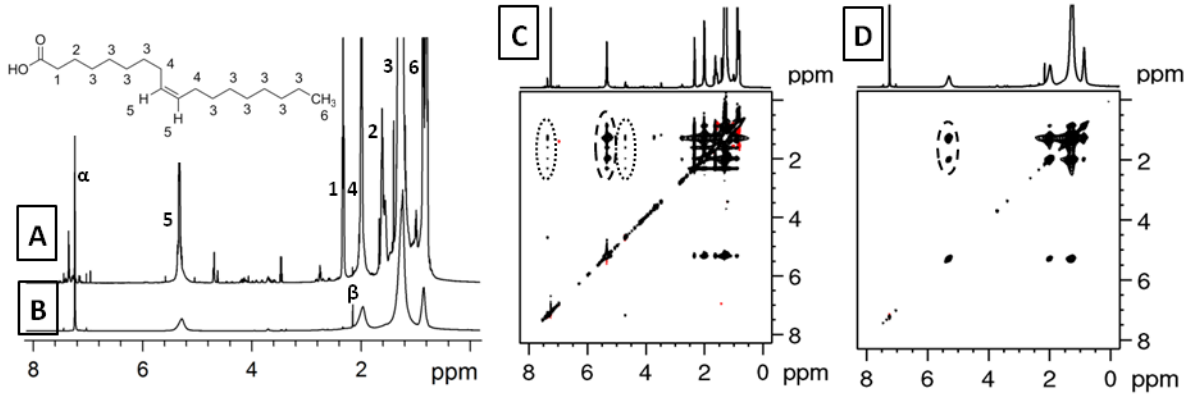

Figure 7. ^{1}H NMR spectra of c-ZrO_2 NCs – starting from the propoxide precursor treated at 230°C for 6h – in $CDCl_3$ stabilized with oleic acid before (spectrum A) and after five (spectrum B) purification steps, concentration = 17 mg ZrO_2 per mL. Greek letters refer to resonances from the solvent and the nonsolvent used during purification. (C) Two-dimensional NOESY spectrum directly obtained after post-modification. (D) Two-dimensional NOESY spectrum after purification.

selected because the well-resolved alkene resonance of OAc strongly facilitates the interpretation in NMR spectra.[47] Two 1D ^{1}H NMR spectra corresponding to samples with c-ZrO_2 NCs treated at 230°C for 6 hours prior to (spectrum A) and after five purifications (spectrum B) are compared in **Figure 7**. Bound ligands typically feature peak broadening due to excessive T_2 relaxation.[47] The resonances at 5.3 ppm are characteristic of the alkene resonance of oleic acid, while their broadening in both spectra and the presence of very clear negative nOe cross-peaks to the methylene resonances of the alkyl chain in the 2D NOESY spectra (dashed circle in **Figure 7**B and C) confirm that OAc is bound to the NCs surface before and after purification.[47] In spectrum A (before purification) a second, sharper resonance is present superimposed upon the broad alkene resonance of bound OAc. Although the narrow width of the peak suggests that this feature corresponds to free OAc, very

clear negative NOE cross-peaks emanating from this resonance can also be observed, indicating the proximity of OAc to the NCs surface in sample A. This particular behavior has already been observed for OAc stabilized CdSe, PbS and HfO_2 nanocrystals and can be explained by equilibria between three states of the fatty acid ligand: bound to the NC, free in solution, and entangled in the ligand shell.[34, 46] Fast exchange between the free and the entangled state results in one sharp single resonance with properties of both. The bound state emerges as a separate broad resonance due to slow exchange with the entangled state. The ^{1}H NMR spectrum of sample A (unpurified NCs, **Figure 7**A) also shows resonances of benzyl alcohol at 4.69, 7.27, 7.35 and 7.35 ppm, see Supporting Information for the assignment. The negative (black) cross peaks in the 2D NOESY spectrum (dotted circles in **Figure 7**C) indicate that benzyl alcohol is spending time at the surface of the NC. However, the resonances are quite narrow and this suggests that that benzyl alcohol is in fast exchange between a bound and a free state, therefore not firmly bound to the surface. The ratio benzyl alcohol-oleic acid is determined as 0.04 (2 mM - 46.35 mM) from ^{1}H NMR integration, which is much lower than the ratio (1.4) reported by Garnweitner *et al.* based on TGA measurements.[22] This difference is probably due to the use of the two different techniques. TGA gives information on the burn-out of all carbon-based molecules and thus also possible impurities, while ^{1}H NMR determines the concentrations of both benzyl alcohol and oleic acid from their specific resonances.

The purified NCs (spectrum B) only show bound oleic acid. Therefore benzyl alcohol, free oleic acid and other impurities (e.g. diethyl ether, ethanol and other unidentified resonances) are removed after additional purification steps. This further advocates the weak binding of benzyl alcohol to the surface.

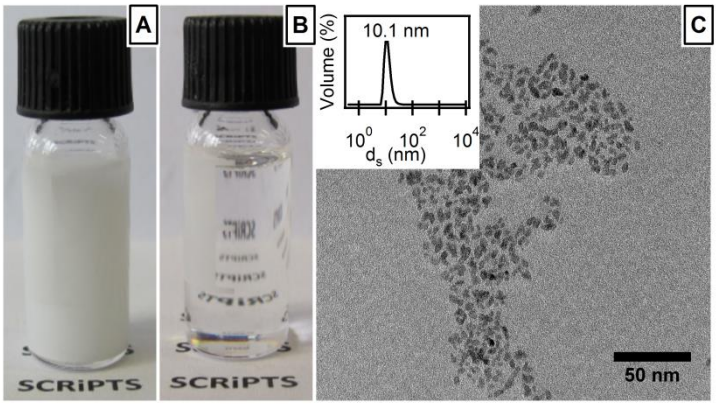

Figure 8. m-ZrO_2 NCs in chloroform before (A) and after (B) post-modification, DLS (C) and TEM (D) analysis of the post-modified m-ZrO_2 NCs starting obtained from the chloride precursor microwave treated at 220°C for 4 hours.

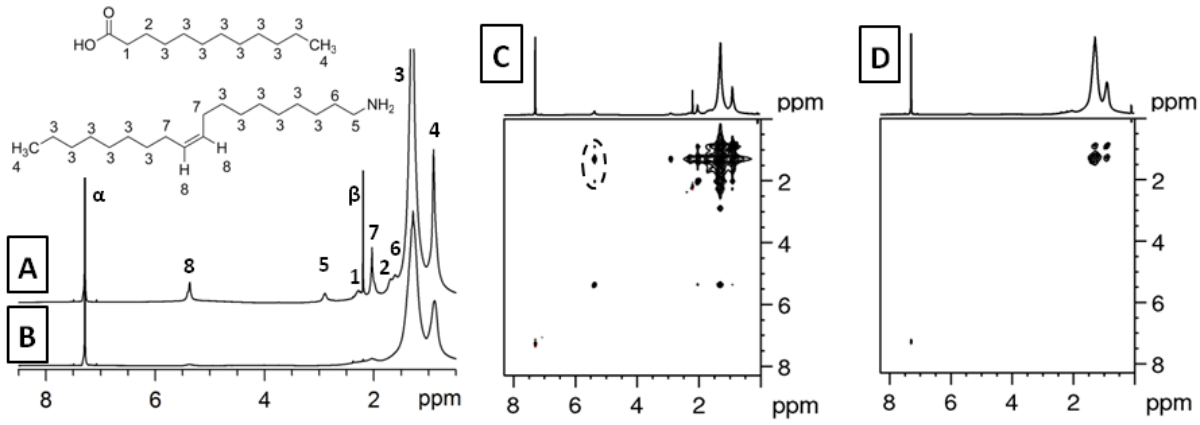

Figure 9. ^{1}H NMR spectra of m-ZrO_2 NCs – starting from the chloride precursor treated at 220°C for 4h – in $CDCl_3$ stabilized with DDAc and OAm after one (spectrum A) and five purification steps (spectrum B), concentration = 56 mg ZrO_2 per mL. Greek letters refer to resonances from the solvent and the nonsolvent used during purification. (C) Two-dimensional NOESY spectrum after five purification steps.

Chloride precursor. The reaction conditions for the chloride precursor were adapted to 220°C and 4 hours. The resulting NCs still retain the monoclinic phase (see Supporting Information), but the yield decreased from 99.5 % to 78.7 %. Due to the milder reaction parameters the m-ZrO_2 NCs are dispersed into the water phase present after synthesis, instead of forming a white precipitate. Subsequent surface functionalization and de-agglomeration proved impossible without this colloidal water phase. As mentioned earlier, the chloride precursor liberates HCl during the reaction and catalyses the condensation of benzyl alcohol to dibenzyl ether and water. The colloidal stability of the particles in the water phase is ensured by their positive charge due the protonation of the NCs surface by HCl.[34] The particles are precipitated from the water phase, washed and dispersed in chloroform leading to a turbid and unstable suspension (**Figure 8**A). Subsequently, a carboxylic acid (oleic acid, dodecanoic acid, …) is added, similar as to the c-ZrO_2 NCs, but the suspensions now remains turbid and unstable. Only the addition of a base (oleyl amine) together with the carboxylic acid resulted in a clear and colorless suspension (**Figure 8**B). DLS analysis in **Figure 8**C confirms that aggregrate-free m-ZrO_2 NCs with an average solvodynamic diameter of 10 nm are obtained after post-modification. TEM analysis shown in **Figure 8**D confirms that the NCs are individual, yet elongated. The long edge of the NCs is ± 7 nm in size, which is in agreement with the solvodynamic diameter determined by DLS.

Again, NMR analysis is used to study the NC-ligand interactions. Spectrum A in **Figure 9** represents the ^{1}H NMR spectrum of ZrO_2 NCs after surface modification with oleylamine (OAm) and dodecanoic acid (DDAc) and a single purification step. Spectrum B originates from a 5 times purified sample. DDAc is used instead of OAc as carboxylic acid, because OAc and OAm have fully overlapping resonances making it difficult to distinguish between both molecules. While this is also the case for the resonances below 2 ppm originating from aliphatic moieties of DDAc and OAm, only OAm shows a characteristic resonance at 5.35 ppm due to its alkene group. This alkene signal drastically decreases in spectrum B, so we can conclude that OAm is almost completely removed after purification, although the molecule is necessary to realize the surface functionalization. In spectrum B bound DDAc is visible, but spectrum A is more difficult to interpret. In that case 2D NOESY NMR is more conclusive to assess ligand binding. Clear negative (black) nOe cross-peaks are visible for the distinct alkene resonance (dashed circle in **Figure 9**C), indicating the proximity of OAm to the NC's surface in spectrum A. The nOe cross-peaks between the aliphatic moieties in **Figure 9**D also confirm that DDAc interacts with the NCs in spectrum B. These results are in line with the observations for HfO_2 NCs synthesized by De Roo *et al.*, where was concluded that oleyl amine removes adsorbed HCl (formed during synthesis) from the surface after which DDAc can dissociate on the ZrO_2 NC surface.[34]

From this we conclude that a different surface functionalization step is necessary to de-aggregate the different crystalline ZrO_2 phases. These results clearly illustrate that the use of a different precursor not only lead to a different reaction mechanism and crystalline phase, but also to a different surface chemistry.

CONCLUSION

In this work, we explored if a microwave-assisted solvothermal method could be used to synthesize crystalline ZrO_2 NCs via the benzyl alcohol route, similar to the conventional solvothermal autoclave method introduced by Niederberger *et al*. We were not only able to obtain high quality ZrO_2 NCs, but we could also reduce the reaction time up to 12 times (2 days vs. 4 hours) by using the more efficient microwave heating technology.

We examined the use of different types of zirconium precursors and found that the reaction mechanism, surface chemistry and crystalline phase are affected if a precursor that is able to release a strong acid is used.

We found that pure m-ZrO_2 NCs are obtained when using $ZrCl_4$, while pure c-ZrO_2 NCs are obtained when using zirconium propoxide, ethoxide and acetate. Mechanistic investigations using GC-MS confirmed that the change in crystal structure comes with a difference in reaction mechanism induced by the release of a strong acid during synthesis. So, we are able to tune the reaction in order to synthesize either pure cubic or monoclinic ZrO_2 NCs, making it possible to use these NCs in crystal phase dependent ZrO_2 applications.

All the as-synthesized ZrO_2 NCs have an average diameter between 3 and 10 nm, yet are aggregated. Aggregate-free NC suspensions can be obtained after a post-modification treatment, dependent on the used precursor during the microwave treatment. The c-ZrO_2 NCs attained from the propoxide precursor are stabilized with a long chain carboxylic acid only, while an additional base is necessary to stabilize the m-ZrO_2 NCs from the chloride precursor. Solution ^{1}H NMR studies confirmed the binding of the carboxylic acid to the NCs and the role of oleyl amine for the m-ZrO_2 NCs from the chloride precursor. It removes adsorbed HCl (formed during synthesis) from the surface after which the carboxylic acid can dissociate on the m-ZrO_2 NC surface. These observations prove the role of the precursor in the determination of the surface chemistry.

ASSOCIATED CONTENT

Supporting information.
Temperature-pressure profiles collected during microwave treatment, GC-MS analysis, characterization of a ZrO_2 suspension via an optimized microwave treatment on the chloride precursor, NMR measurements on the propoxide precursor treated at 270°C-4h and assignments of benzyl alcohol in the NMR spectra of the ZrO_2 obtained from the chloride precursor. This material is available free of charge via the Internet at http://pubs.acs.org.

AUTHOR INFORMATION

Corresponding Author

Isabel.VanDriessche@ugent.be

Notes

The authors declare no competing financial interest.

ACKNOWLEDGMENTS

We would like to express our gratitude to Jan Goeman for GC-MS measurements. K.D.K. acknowledges UGent for funding (BOF project), J.D.R. acknowledges FWO Vlaanderen for funding. The NMR equipment used was fonded through a grant from the Hercules foundation.

ABBREVIATIONS

NC, nanocrystal; BnOH, benzyl alcohol; TFA, trifluoroacetic acid; OAc, oleic acid, OAm, oleyl amine; DDAc, dodecanoic acid.

REFERENCES

(1) Gallino, F.; Di Valentin, C.; Pacchioni, G. *Phys. Chem. Chem. Phys.* **2011**, *13*, 17667-17675.

(2) Cheema, T.A.; Garnweitner, G. *Crystengcomm* **2014**, *16*, 3366-3375.

(3) He, D.; Ding, Y.; Luo, H.; Li, C. *J. Mol. Catal. A-Chem.* **2004**, *208*, 267-271.

(4) Joo, J.; Yu, T.; Kim, Y.W.; Park, H.M.; Wu, F.; Zhang, J.Z.; Hyeon, T. *J. Am. Chem. Soc.* **2003**, *125*, 6553-6557.

(5) Siddiqui, M.R.H.; Al-Wassil, A.I.; Al-Otaibi, A.M.; Mahfouz, R.M. *Mat. Res.* **2012**, *15*, 986-989.

(6) Stichert, W.; Schüth, F.; Kuba, S.; Knözinger, H. *J. Catal.* **2001**, *198*, 277-285.

(7) Wang, G.C.; Meng, F.H.; Ding, C.X.; Chu, P.K.; Liu, X.Y. *Acta Biomater.* **2010**, *6*, 990-1000.

(8) Wilk, G.D.; Wallace, R.M.; Anthony, J.M. *J. Appl. Phys.* **2001**, *89*, 5243-5275.

(9) Xu, X.X.; Wang, X. *Nano Res.* **2009**, *2*, 891-902.

(10) Clearfield, A. *Inorg. Chem.* **1964**, *3*, 146-148.

(11) Garvie, R.C. *J. Phys. Chem.* **1965**, *69*, 1238-1243.

(12) Tang, J.; Zhang, T.; Zoogman, P.; Fabbri, J.; Chan, S.W.; Zhu, Y.M.; Brus, L.E.; Steigerwald, M.L. *Adv. Funct. Mater.* **2005**, *15*, 1595-1602.

(13) Garvie, R.C. *J. Phys. Chem.* **1978**, *82*, 218-224.

(14) Bondioli, F.; Corradi, A.B.; Ferrari, A.M.; Leonelli, C. *J. Am. Ceram. Soc.* **2008**, *91*, 3746-3748.

(15) Hwang, S.M.; Choi, J.H.; Lee, S.M.; Lim, J.H.; Joo, J. *J. Phys. Chem. C* **2012**, *116*, 11386-11392.

(16) Li, W.Z.; Huang, H.; Li, H.J.; Zhang, W.; Liu, H.C. *Langmuir* **2008**, *24*, 8358-8366.

(17) Liang, J.H.; Deng, Z.X.; Jiang, X.; Li, F.L.; Li, Y.D. *Inorg. Chem.* **2002**, *41*, 3602-3604.

(18) Rao, K.J.; Mahesh, K.; Kumar, S. *B. Mater. Sci.* **2005**, *28*, 19-24.

(19) Singh, A.K.; Nakate, U.T. *ScientificWorldJournal* **2014**,

(20) Hernawan, R.S.; Sofiyaningsih, N.; Sutardi, S. *J. Ceram. Process. Res.* **2011**, *12*, 561-566.

(21) Zhao, N.N.; Pan, D.C.; Nie, W.; Ji, X.L. *J. Am. Chem. Soc.* **2006**, *128*, 10118-10124.

(22) Garnweitner, G.; Goldenberg, L.M.; Sakhno, O.V.; Antonietti, M.; Niederberger, M.; Stumpe, J. *Small* **2007**, *3*, 1626-1632.

(23) Garnweitner, G.; Niederberger, M. *J. Am. Ceram. Soc.* **2006**, *89*, 1801-1808.

(24) Niederberger, M.; Garnweitner, G.; Pinna, N.; Antonietti, M. *J. Am. Chem. Soc.* **2004**, *126*, 9120-9126.

(25) Pinna, N.; Niederberger, M. *Angew. Chem.-Int. Edit.* **2008**, *47*, 5292-5304.

(26) De Keukeleere, K.; Feys, J.; Meire, M.; De Roo, J.; De Buysser, K.; Lommens, P.; Van Driessche, I. *J. Nanopart. Res.* **2013**, *15*, 2074.

(27) De Roo, J.; De Keukeleere, K.; Feys, J.; Lommens, P.; Hens, Z.; Van Driessche, I. *J. Nanopart. Res.***2013**, *15*, 1778.

(28) Shi, S.; Hwang, J.-Y. *Journal of Minerals & Materials Characterization & Engineering* **2003**, *2*, 101-110.

(29) Niederberger, M.; Garnweitner, G. *Chem.-Eur. J.* **2006**, *12*, 7282-7302.

(30) Niederberger, M.; Garnweitner, G.; Pinna, N.; Neri, G. *Prog. Solid State Ch.* **2005**, *33*, 59-70.

(31) Pinna, N.; Garnweitner, G.; Antonietti, M.; Niederberger, M. *Adv. Mater.* **2004**, *16*, 2196-2200.

(32) Niederberger, M.; Garnweitner, G.; Krumeich, F.; Nesper, R.; Colfen, H.; Antonietti, M. *Chem. Mater.* **2004**, *16*, 1202-1208.

(33) Obradors, X.; Puig, T.; Palau, A.; Pomar, A.; Sandiumenge, F.; Mele, P.; Matsumoto, K. *Comprehensive Nanoscience and Technology* **2011**, 303-349.

(34) De Roo, J.; Van den Broeck, F.; De Keukeleere, K.; Martins, J.C.; Van Driessche, I.; Hens, Z. *J. Am. Chem. Soc.* **2014**, *136*, 9650-9657.

(35) Grote, C.; Cheema, T.A.; Garnweitner, G. *Langmuir* **2012**, *28*, 14395-14404.
(36) Pinna, N.; Grancharov, S.; Beato, P.; Bonville, P.; Antonietti, M.; Niederberger, M. *Chem. Mater.* **2005**, *17*, 3044-3049.
(37) Zhou, S.X.; Garnweitner, G.; Niederberger, M.; Antonietti, M. *Langmuir* **2007**, *23*, 9178-9187.
(38) Connell, M.A.; Bowyer, P.J.; Bone, P.A.; Davis, A.L.; Swanson, A.G.; Nilsson, M.; Morris, G.A. *J. Magn. Reson.* **2009**, *198*, 121-131.
(39) Sinnaeve, D. *Concepts Magn. Reson. A* **2012**, *40A*, 39-65.
(40) Leger, J.M.; Tomaszewski, P.E.; Atouf, A.; Pereira, A.S. *Phys. Rev. B* **1993**, *47*, 14075-14083.
(41) Ozturk, H.; Durandurdu, M. *Phys. Rev. B* **2009**, *79*, 134111
(42) Taguchi, M.; Nakane, T.; Matsushita, A.; Sakka, Y.; Uchikoshi, T.; Funazukuri, T.; Naka, T. *J. Supercrit. Fluid* **2014**, *85*, 57-61.
(43) Stefanic, G.; Music, S.; Molanov, K. *J. Alloy Compd* **2005**, *387*, 300-307.
(44) Taguchi, M.; Takami, S.; Adschiri, T.; Nakane, T.; Sato, K.; Naka, T. *Crystengcomm* **2012**, *14*, 2132-2138.
(45) Taguchi, M.; Takami, S.; Adschiri, T.; Nakane, T.; Sato, K.; Naka, T. *Crystengcomm* **2012**, *14*, 2117-2123.
(46) Fritzinger, B.; Capek, R.K.; Lambert, K.; Martins, J.C.; Hens, Z. *J. Am. Chem. Soc.* **2010**, *132*, 10195-10201.
(47) Hens, Z.; Martins, J.C. *Chem. Mater.* **2013**, *25*, 1211-1221.
(48) Sato, K.; Abe, H.; Ohara, S. *J. Am. Chem. Soc.* **2010**, *132*, 2538-2539.

TOC